Low-temperature pyroelectricity of a saccharose single crystal

Jacques Mangin and Armand Hadni*
University of Nancy-I 54037 Nancy-Cedex, France
(Received 16 May 1977)

The pyroelectric response of a saccharose single crystal is hardly detectable at room temperature but shows a maximum at 14 K (pyroelectric coefficient $\pi' \simeq 2 \times 10^{-4}$ $\mu C/cm^2K$). The low-temperature behavior is explained in terms of the lower-frequency TO phonons involving an electric-dipole variation, parallel to the pyroelectric axis ($\dot{\nu} = 45$ cm^{-1}). There is no hint of the so-called Born divergence down to 5 K.

I. INTRODUCTION

Pyroelectric detectors have been developed for several years.[1] They are generally used at room temperature. However, it has been suggested that the pyroelectric response could diverge at very low temperature[2,3] and we would like to discuss this rather complicated problem in the case of saccharose which belongs to a pyroelectric crystalline system at room temperature ($C_2^2 - P_{2_1}$) and the pyroelectricity of which has been quoted by Hayashi.[4]

For pyroelectric measurements, the electric displacement vector $\vec{D} = \epsilon_0 \vec{E} + \vec{P}$ is of the most importance since it gives the charge density on the plane-parallel faces of the electrodes in a classic condenser generally used for such experiments. D is defined in terms of electric field E and polarization P, and it is this charge density which is the purpose of the measurements. In the case of vacuum $P = 0$, and $D = \epsilon_0 E$, with $E = -V/d$ (Fig. 1), V being an external potential applied to the plates; when a dielectric is filling the empty space between both electrodes, the charge density is increased by P (Fig. 2): $D = \epsilon_0 E + P$.

Now, if there is no external potential applied to the plates (Fig. 3), $E = 0$ and the charge density is written $D = P$. It is null except in the case of spontaneous polarization P_s. Let us consider a pyroelectric plate cut perpendicular to the polar axis: $P = P(T, E, \sigma)$, σ being the macroscopic stress tensor, and hence, $D = D(T, E, \sigma)$. On the other hand, σ is related to the strain tensor s, $\sigma = \sigma(s, T)$, and $D = D(T, E, s)$. It will be understood that in all the differentiations the macroscopic electric field is kept constant and that this constant value is zero, or close to zero (cf. Fig. 3). Then,

$$dD = \left(\frac{\partial D}{\partial T}\right)_s dT + \left(\frac{\partial D}{\partial s}\right)_T ds;$$

now

$$ds = \left(\frac{\partial s}{\partial T}\right)_\sigma dT + \left(\frac{\partial s}{\partial \sigma}\right)_T d\sigma,$$

$$dD = \left(\frac{\partial D}{\partial T}\right)_s dT + \left(\frac{\partial D}{\partial s}\right)_T \left[\left(\frac{\partial s}{\partial T}\right)_\sigma dT + \left(\frac{\partial s}{\partial \sigma}\right)_T d\sigma\right],$$

$$dD_\sigma = \left(\frac{\partial D}{\partial T}\right)_s dT_\sigma + \left(\frac{\partial D}{\partial s}\right)_T \left(\frac{\partial s}{\partial T}\right) dT_\sigma,$$

$$\left(\frac{\partial D}{\partial T}\right)_\sigma = \left(\frac{\partial D}{\partial T}\right)_s + \left(\frac{\partial D}{\partial s}\right)_T \left(\frac{\partial s}{\partial T}\right)_\sigma.$$

The left-hand side gives the "total pyroelectric coefficient" (constant stress)

$$\left(\frac{\partial D}{\partial T}\right)_\sigma = \left(\frac{\partial P_s}{\partial T}\right)_\sigma = \pi. \tag{1}$$

The first term in the right-hand side gives what is called the "primary pyroelectric coefficient" (constant strain)

$$\left(\frac{\partial D}{\partial T}\right)_s = \left(\frac{\partial P_s}{\partial T}\right)_s = \pi_1. \tag{2}$$

The second term gives the secondary pyroelectric coefficient

$$\left(\frac{\partial D}{\partial s}\right)_T \left(\frac{\partial s}{\partial T}\right)_\sigma = \left(\frac{\partial P_s}{\partial s}\right)_T \left(\frac{\partial s}{\partial T}\right)_\sigma = \pi_2$$

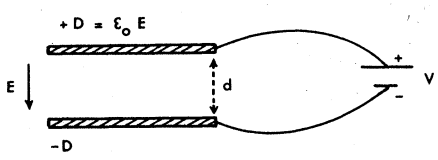

FIG. 1. Vector displacement D in a vacuum condenser.

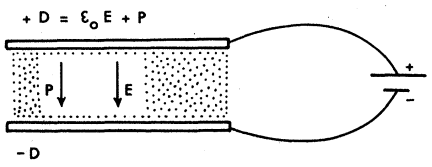

FIG. 2. Vector displacement D in a dielectric condenser.

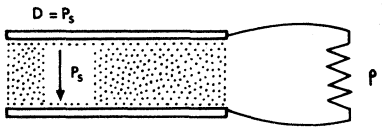

FIG. 3. Vector displacement D in a dielectric condenser (no external electric field applied).

and

$$\pi = \pi_1 + \pi_2 . \tag{3}$$

Now,

$$\pi_2 = \left(\frac{\partial P_s}{\partial \sigma}\right)_T \left(\frac{\partial \sigma}{\partial s}\right)_T \left(\frac{\partial s}{\partial T}\right)_\sigma ;$$

$\pi_2 = d_{3i} c_{ij} \alpha_j$, where $i,j = 1, 2, 3$ label coordinate directions, with direction 3 parallel to the spontaneous polarization, d_{3i} are piezoelectric compliances, c_{ij} are elastic moduli, and α_j are the thermal expansion coefficients. It is seen that π_2 is induced by expansion via the piezoelectric effect.

According to Glass *et al.*,[5] if we look more closely at the unclamped experimental condition, in the expanded situation at temperature $T + dT$, the condenser charge Q will adjust itself to $Q + dQ$ in such a way that it again cancels the total displacement charge, i.e.,

$$Q + dQ = \frac{\mu(T + dT)}{(1 + \alpha_3 dT)\, d} ,$$

$\mu(T + dT)$ being the total electric dipole value at $T + dT$.

$$Q + dQ = \frac{(P_s + dP_s) A d (1 + 2\alpha_1 dT + \alpha_3 dT)}{d(1 + \alpha_3 dT)} .$$

Hence

$$dQ \simeq 2 A P_s \alpha_1 dT + A\, dP_s .$$

Now we measure

$$dP_s' = (dQ/A) = dP_s + 2 P_s \alpha_1 dT ,$$

and thus

$$-\left(\frac{\partial P_s'}{\partial T}\right)_\sigma = \pi - 2 P_s \alpha_1 .$$

Let us write $\pi' = -(\partial P_s' / \partial T)_\sigma$, the "apparent" pyroelectric coefficient, and then

$$\pi' = \pi_1 + \pi_2 - 2 P_s \alpha_1 . \tag{4}$$

The "apparent" pyroelectric coefficient π' we measure with an unclamped sample is the sum of the clamped or primary pyroelectric coefficient, plus the secondary pyroelectric coefficient due to thermal expansion via the piezoelectric effect ($\pi_2 = d_{3i} c_{ij} \alpha_j$), plus a term due to pure thermal expansion in directions perpendicular to the polar axis. Now, at very low temperature, $\alpha_j \propto T^3$, $P_s \simeq$ const, then

$$\pi' \simeq \pi_1 + K T^3 . \tag{5}$$

Now we are able to limit the discussion to the temperature behavior of π_1; the primary pyroelectric coefficient (clamped pyroelectricity). This discussion is of great interest both theoretically and for its practical application to pyroelectric detectors. From a theoretical point of view π_1 occurs from the anharmonicity of lattice vibration and this has been first discussed by Born in 1945[2] and in 1954.[6] In this last discussion, it has been shown that π_1 is proportional to T^3 at very low temperature. A simplified demonstration has been given by Grout *et al.*[3] in the case of a one-dimensional anharmonic oscillator with potential energy $V(z) = \frac{1}{2} a z^2 + \frac{1}{3} b z^3$. The z^3 term is present only in the noncentrosymmetric case required for pyroelectricity. The condition of equilibrium, $\partial V / \partial z = 0$, yields $az = -bz^2$, and if we accept it for small vibrations, then

$$\langle z \rangle = -(b/a) \langle z^2 \rangle . \tag{6}$$

Then a rigid-ion model is assumed. The electronic clouds follow the ions without deformation, and hence the average dipole moment $\langle p \rangle$ of the oscillator is proportional to $\langle z \rangle$, and thus $\langle p \rangle \propto E$, E being the average energy of the lattice oscillator, proportional to T^4 at low temperature. We thus have $\pi_1 \propto T^3$. Szigeti[7] has given a general demonstration and rejected the first arguments of Born,[2] leading to a linear relation between π_1 and T in all cases, and those of Grout *et al.*,[3] leading to the same linearity for nonrigid ions. Szigeti has shown that π_1 is proportional to T^3 near absolute zero, and that the cubic potential and second-order moment enter into π_1 in exactly the same way and with the same temperature dependence.

From an experimental point of view the earlier experimental measurements by Ackerman[8] are the only ones which could be in favor of this linearity. But in fact they were only made at 23 and 88 K. For ZnO studied between 4 and 300 K, π_1 is proportional to T^3.[9] For lithium sulphate monohydrate, the pyroelectric coefficient shows a change of sign at about 110 K.[10] To account for this behavior, Lang extended the Born theory by adding a contribution from nondispersive optical modes to the pyroelectric effect. Agreement between theory and experiment was obtained with five independent oscillators in addition to the acoustical modes, by adjusting the coefficients and frequencies to fit the pyroelectric and specific-heat data. In fact, while ZnO has only one ir-active band located at a high frequency (380 cm^{-1}), $LiSO_4 \cdot H_2O$ has a number of low-frequency ir-active bands.

However, the frequencies used by Lang have not been correlated to the far-ir–active bands. There is also the case of $LiNbO_3$ and $LiTaO_3$ where measurements have been reported[5] from above room temperature down to 5 K. In a remarkable paper,[5] they are explained mainly by the contribution of one far-ir lattice vibration, but its frequency (around 65 cm^{-1} in both materials) is somewhat different from the soft modes. This lattice vibration gives rise to a pronounced maximum in the pyroelectric response (proportional to $\pi'/\mathcal{C}$, $\mathcal{C}$ being the heat capacity) which is observed near 30 K.

We shall see the same effect in the case of saccharose where a maximum is observed at 14 K, but in that case the lattice vibration responsible for it corresponds to the strongest far-ir absorption band located at 45.4 cm^{-1}. [A maximum has also been observed for the pyroelectric response of $NdBrO_3 \cdot 9H_2O$. It is located at 61.5 K. However it is a sharp maximum and it has been explained by a phase transition.[11] We shall exclude these cases where heating produces phase transitions.]

II. EXPERIMENTAL

A. Charge-integration technique

The change of spontaneous polarization as a function of temperature was obtained by integrating the charge which appears on the faces of the crystal with an operational amplifier.[11,12] With this arrangement the field across the crystal is essentially zero at all times, and the polarization change can be recorded continuously as a function of temperature. The crystals were $5\times5\times0.3$ mm^3 and electroded with silver paste on the faces normal to the polar axis and fixed to the copper finger of the cryostat. The temperature is given by an AsGa diode located in a hole behind the crystal (Fig. 4). A glue improves the thermal contact between the diode and the holder. The distance between diode and pyroelectric plate is kept smaller than 0.5 mm.

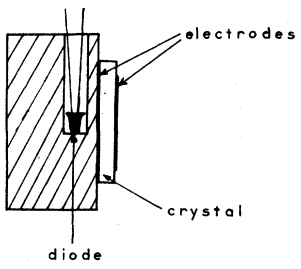

FIG. 4. Crystal plate mounted with silver glue on a copper finger.

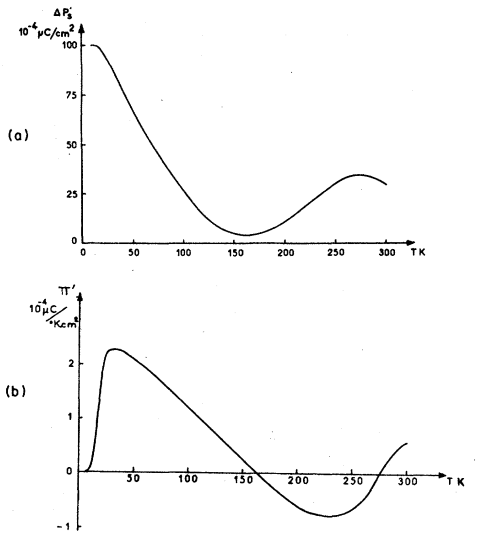

FIG. 5.(a) $\Delta P_s'$ vs T obtained by the charge-integration technique. (b) π' vs T derived from Fig. 5.

The change $\Delta P_s'$ of spontaneous polarization versus temperature is given in Fig. 5(a) from 6 to 300 K, and $\pi' = -d(\Delta P_s')/dT$ is also calculated [Fig. 5(b)]. There is a change of sign around 160 and 270 K.

B. Dynamic pyroelectric technique

This method, first developed by Chynoweth[13] does not give directly the pyroelectric coefficient π and has to be used with some care.[14] Let us re-

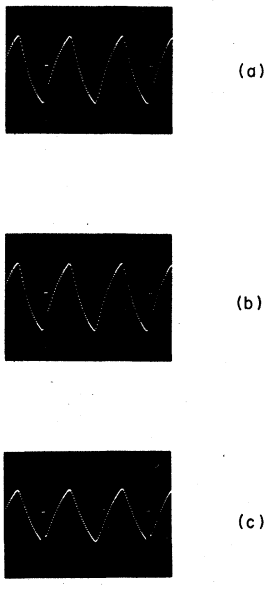

FIG. 6. Pyroelectric signal at 800 Hz for $T = 6$ K (a), $T = 20$ K (b), $T = 30$ K (c).

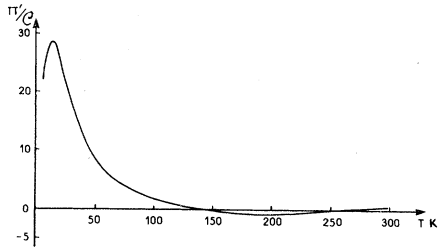

FIG. 7. Pyroelectric response π_1/c vs T (experimental). The unit is 10^{-6} μC/J K.

call the result of a simple treatment of a pyroelectric detector.[15] The pyroelectric plate perpendicular to the pyroelectric axis (type-I detector) is short-circuited by a bias resistance ρ and is illuminated on its whole surface by a beam sine wave modulated at an angular frequency ω.

A sine-wave voltage at the same frequency appears across the crystal with amplitude

$$S = E\Delta L_M \alpha \mathcal{T} R \tfrac{1}{2}\omega\pi'(1+\omega^2\tau^2)^{-1/2} \times (1+\omega^2\tau'^2)^{-1/2}, \tag{7}$$

where ΔL_M is the amplitude of brightness modulation; E is the beam acceptance; α is the absorption coefficient of the detector; $\mathcal{T}$ is the window transmission; $\pi' = -(dP_s')/dT$ is the apparent pyroelectric coefficient; g is the thermal conductance per unit area; $\tau = c/g$ is the thermal time constant; c is the thermal capacity per unit square area ($c = c'd$, c' being the thermal capacity per unit volume); $R^{-1} = \rho^{-1} + (\rho')^{-1}$, ρ being the bias resistance, ρ' the internal resistance of the crystal plate, and $\tau' = RC$ is the electrical time resistance, C being the electrical capacity. Let us assume $\omega^2\tau'^2 \ll 1$ and $\omega^2\tau^2 \gg 1$, then

$$S \simeq \tfrac{1}{2} E\Delta L_M \alpha \mathcal{T} R(\pi'/c). \tag{8}$$

To satisfy these conditions we had to use a chopper at a 800-Hz frequency. The light source is a He-Ne laser ($\lambda = 6328$ Å), the brilliancy of it being suitably attenuated; the bias resistance $\rho = 10^{11}$ Ω.

The signal from the pyroelectric detector is amplified with a PAR amplifier No. 121. Its shape is continuously visualized on a cathode ray oscilloscope through a wave form eductor PAR No. TDH9. The wave shape is still a triangle at temperatures as low as 6–20 and 30 K (Fig. 6).

The result of the study is given in Fig. 7 in terms of π'/c versus temperature from 6 to 300 K. There is a maximum for $T = 14$ K, a change of sign at 150 and 260 K, and the pyroelectric response is close to zero above 140 K.

III. THEORY

A. General treatment

Following Garrett[16] we shall use a model with one single-anharmonic optical mode giving a dipole-moment variation parallel to the polar axis z. Let us call $\vec{p}_l$ the electric dipole moment of the lth primitive unit cell of the pyroelectric crystal.

Its direction is parallel to the polar axis z and its modulus is temperature dependent. In the unit-cell number l, the displacement of the atoms in a vibrational mode giving a dipole-moment variation parallel to z depends on an Hamiltonian H_l, which can be written simply in the case of one coordinate variation

$$H_l = m_l^2/2\mu + \tfrac{1}{2}\mu\omega^2 z_l^2 + \alpha z_l^3 + \beta z_l^4. \tag{9}$$

μ is the reduced mass, m_l the momentum, z_l the displacement along the z axis; α and β are anharmonic coefficients (the α coefficient is introduced in the case of pyroelectric crystals where there is a lack of center of symmetry).

For this anharmonic oscillator we can include the quartic term to first order and the cubic term to second order in perturbation theory.[17] In that approximation, the energy levels are written

$$E_v = \hbar\omega(v+\tfrac{1}{2}) - \frac{15}{4}\frac{\alpha^2}{\hbar\omega}\left(\frac{\hbar}{\mu\omega}\right)^3 (v^2+v+\tfrac{11}{30}) + \tfrac{3}{2}\beta\left(\frac{\hbar}{\mu\omega}\right)^2 (v^2+v+\tfrac{1}{2}). \tag{10}$$

Let us assume that the temperature is low enough to confine practically all oscillators population in levels 0-1-2 (Fig. 8); then

$$\bar{E} \simeq \frac{d}{d(1/kT)} \sum_{v=0}^{2} e^{-E_v/kT} \left(\sum_0^2 e^{-E_v/kT}\right)^{-1},$$

$$\bar{E} \simeq \frac{A + (A+A_1-2A_2)\,e^{-(A_1-2A_2)/kT} + (A+2A_1-6A_2)\,e^{-(2A_1-6A_2)/kT}}{1 + e^{-(A_1-2A_2)/kT} + e^{-(2A_1-6A_2)/kT}}, \tag{11}$$

with

$$A = \frac{\hbar\omega}{2} - \frac{15}{4}\frac{\alpha^2}{\hbar\omega}\left(\frac{\hbar}{\mu\omega}\right)^3 \frac{11}{30} + \frac{3}{2}\beta\left(\frac{\hbar}{\mu\omega}\right)^2 \frac{1}{2}, \qquad A_1 = \hbar\omega, \quad A_2 = \frac{15}{4}\frac{\alpha^2}{\hbar\omega}\left(\frac{\hbar}{\mu\omega}\right)^3 - \frac{3}{2}\beta\left(\frac{\hbar}{\mu\omega}\right)^2;$$

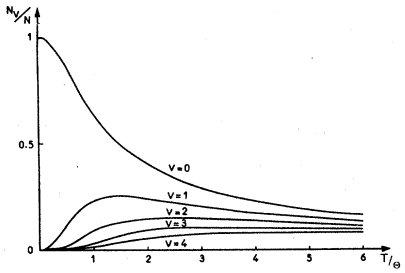

FIG. 8. N_v/N vs T/Θ for a harmonic oscillator.

and to first-order approximation,

$$\bar{E} = A + (A_1 - 2A_2)\, e^{-(A_1-2A_2)/kT}. \tag{12}$$

We can check that in the harmonic-oscillator limit case, i.e., $\alpha = \beta = 0$, $A_2 = 0$, $A \simeq \frac{1}{2}(\hbar\omega)$, we get

$$\bar{E} = \tfrac{1}{2}(\hbar\omega) + \hbar\omega e^{-\hbar\omega/kT}.$$

Now let us assume the average value $\langle \Delta p_l \rangle$ is proportional to $\langle z_l^2 \rangle$ because of anharmonicity and also because electronic clouds deformation gives a second-order dipole contribution (see for instance Refs. 5 and 2);

$$\frac{\langle \Delta p_l \rangle - \langle \Delta p_l \rangle_0}{\langle \Delta p_l \rangle_0} = \frac{\langle z_l^2 \rangle - \langle z_l^2 \rangle_0}{\langle z_l^2 \rangle_0}. \tag{13}$$

$\langle \Delta p_l \rangle_0$ being the contribution of one mode of the TO branch to the electric dipole moment at 0 K. Now, for the harmonic oscillator,

$$\langle z_l^2 \rangle = \bar{E}/\omega^2. \tag{14}$$

Accepting this relation as a first approximation for the anharmonic oscillator, we write

$$\frac{\langle \Delta p_l \rangle - \langle \Delta p_l \rangle_0}{\langle \Delta p_l \rangle_0} \simeq \frac{(A_1 - 2A_2) e^{-(A_1-2A_2)/kT}}{A},$$
$$\langle \Delta p_l \rangle \simeq \langle \Delta p_l \rangle_0 \left(\frac{(A_1 - 2A_2)}{A} e^{-(A_1-2A_2)/kT} + 1 \right). \tag{15}$$

In fact, the primitive unit-cell l is not isolated in the crystal and its energy results from its participation to all modes of the optical branch. If we neglect any dispersion of the TO branch, all modes have the same frequency and the average vibrational energy of the lth unit cell due to the TO branch considered above is the total energy of all modes divided by the number of modes (i.e., $h\nu/(e^{h\nu/kT} - 1) + \frac{1}{2}h\nu$ in the harmonic approximation).

In that way, Eq. (15) represents the average dipole moment of the unit cell due to all modes in the TO branch. Now summing on all unit cells contained in the unit volume at 0 K, we get

$$\Delta P_s = \left(\frac{A_1 - 2A_2}{A} e^{-(A_1-2A_2)/kT} + 1 \right) \sum_l \langle \Delta p_l \rangle_0,$$
$$\Delta P_s = \Delta P_{s0} \left(\frac{A_1 - 2A_2}{A} e^{-(A_1-2A_2)/kT} + 1 \right). \tag{16}$$

ΔP_{s0} being the contribution of the whole TO branch to the spontaneous polarization at 0 K and ΔP_s the same contribution at temperature T (neglecting the change of volume).

In a first approximation, neglecting $2A_2$ against A_1, we get

$$A_2 \simeq 0; \quad A \simeq \tfrac{1}{2}\hbar\omega$$

and

$$\Delta P_s \simeq 2\Delta P_{s0}(1+\epsilon) e^{-\hbar\omega/kT} + \Delta P_{s0} \tag{17}$$

with

$$\epsilon = -\frac{19}{4}\left(\frac{\alpha}{\hbar\omega}\right)^2 \left(\frac{\hbar}{\mu\omega}\right)^3 + \frac{1}{2}\frac{\beta}{\hbar\omega}\left(\frac{\hbar}{\mu\omega}\right)^2, \tag{18}$$

$$\pi_1 \simeq -\frac{d}{dT}(\Delta P_s), \quad \pi_1 \simeq 2\Delta P_{s0}(1+\epsilon)\frac{\hbar\omega}{kT^2} e^{-\hbar\omega/kT}.$$

ϵ is thus representing the effect of anharmonicity of the optical mode ω on π_1. This is the same exponential law as obtained by Glass and Lines[5] in a slightly different way.

In the case of saccharose we have used Eq. (18) and assuming $\mathcal{C} = KT^3$ and $\epsilon = 0$, we get

$$\frac{\pi_1}{\mathcal{C}} = \frac{2\Delta P_{s0}\hbar\omega}{kKT^5} e^{-\hbar\omega/kT}. \tag{19}$$

There is a maximum for $d/dt(\pi_1/\mathcal{C}) = 0$, i.e., $T_{\max} = \frac{1}{5}\Theta$, $\Theta = \hbar\omega/k$ being the Einstein temperature of the optical mode.

B. Application to saccharose

The lower far-infrared frequency observed in the absorption spectrum of saccharose has been located at 45.4 cm^{-1} for $T = 4$ K.[18] The band is a strong one, but the polarization is not known since Yoshinaga has not prepared the single crystal and has used the powder. We introduce this frequency in (19) and draw Fig. 9 which is closely related to Fig. 7 (experimental); the maxima of both curves fit remarkably well (theoretical maximum at 13.2 K, observed at 14 K). However we have to insist on the point that the approximations used do not allow to consider the curve drawn on

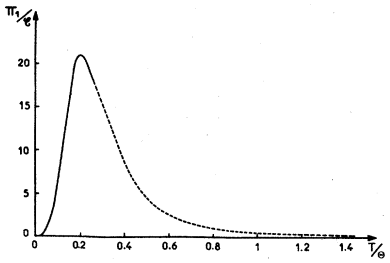

FIG. 9. $\pi_1/\mathcal{C}$ vs T/Θ (theoretical).

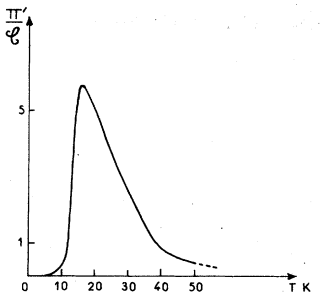

FIG. 10. $\pi'/\mathcal{C}$ vs T derived from 5(b) assuming $\mathcal{C} = KT^3$ (arbitrary units).

Fig. 9 as available for $T/\Theta > 0.3$ and indeed it is drawn as a dotted line.

The experimental curve (Fig. 7) obtained with the dynamic pyroelectric technique can be checked by the charge integration technique which has led to Fig. 5(b) which gives π' vs T. To get $\pi'/\mathcal{C}$ vs T we have to make an assumption on $\mathcal{C}$ since no measurements are available at low temperature. We have put $\mathcal{C} = KT^3$ and drawn Fig. 10 (arbitrary units). A maximum is observed around 16.5 K, which is quite good.

IV. CONCLUSION

The pyroelectricity of saccharose is negligible at room temperature and the low-temperature maximum is very small. The high-sensitivity methods used are needed to make such studies.

However, the pyroelectric method leads to a reasonable signal-to-noise ratio and brings confirmation to the measurements made by others on materials with a much higher pyroelectric coefficient, i.e., $LiSO_4 \cdot H_{20}$, $LiTaO_3$, $LiNbO_3$ where a maximum of the ratio $\pi_1/\mathcal{C}$ has been observed at low temperature. This seems an evidence of the role played by low-frequency transverse optical (TO) phonons when they have the right polarization to give an electric dipole variation parallel to the polar axis. The second-order dipole moment seems responsible for a large part of the low-temperature pyroelectricity. In the case of saccharose, other contributions are negligible and the room-temperature pyroelectricity is hardly detectable. It is the first time that a TO phonon frequency used to explain the pyroelectricity is exactly related to a far-infrared absorption band. We have to check that its polarization is parallel to the polar axis.[19] At very low temperature the contribution of the optical mode to π' is vanishing exponentially [Fig. 5(b)] and we can say there is not any hint of the so-called Born divergence in good accordance with (5) and (7), and we can even state that the term proportional to T^3 in Eq. (3) is very small (Fig. 7).

At high temperature, the pyroelectric response $\pi'/\mathcal{C}$ is close to zero (Fig. 7). There is still a contribution of the lower-frequency polar modes, but formula,[18] which gives positive contributions, is not applicable. On the other hand, $\pi' = \pi_1 + d_{3i} c_{ij} \alpha_j - 2P_s \alpha_1$, and the expansion coefficients are increasing with temperature.

ACKNOWLEDGMENT

We are grateful to Dr. Wyncke for growing the saccharose crystal.

---

*Equipe de Recherche Associée au Centre National de la Recherche Scientifique. No. 14.

[1] A. Hadni, J. Phys. 24, 694 (1963).
[2] M. Born, Rev. Mod. Phys. 17, 245 (1945).
[3] P. J. Grout, N. H. March, and T. L. Thorp, J. Phys. C 8, 2167 (1975).
[4] F. Hayashi, Dissertation (Göttingen, 1912) (unpublished).
[5] A. M. Glass and M. E. Lines, Phys. Rev. B 13, 180 (1976).
[6] M. Born and K. Huang, *Dynamical Theory of Crystal Lattices* (Clarendon, Oxford, England, 1954).
[7] B. Szigeti, Phys. Rev. Lett. 35, 1532 (1975).
[8] W. Ackermann, Ann. Phys. (Leipzi) 46, 197 (1915).
[9] G. Heiland and H. Ibach, Solid State Commun. 4, 353 (1966).
[10] S. B. Lang, Phys. Rev. B 4, 3603 (1971).
[11] H. Poulet, J. P. Mathieu, D. Vergnat, P. Vergnat, A. Hadni, and X. Gerbaux, Phys. Status. Solidi A 32, 509 (1975).
[12] A. M. Glass, J. Appl. Phys. 40, 4699 (1969).
[13] A. G. Chynoweth, J. Appl. Phys. 27, 78 (1956).
[14] A. Hadni, *Essentials of Modern Physics, Appplied to the Study of the Infrared* (Pergamon, New York, 1967).
[15] A. Hadni, IEEE Trans. Microwave Theor. Tech. 22, 1016 (1974).
[16] C. B. G. Garrett, IEEE J. Quantum Electron., 4, 70 (1968).
[17] L. Landau, E. Lifchitz, *Mecanique Quantique* (MIR, Moscow, 1967).
[18] M. Hineno and H. Yoshinaga, Spectrochim. Acta A 30, 411 (1974).
[19] B. Wyncke, J. Serrier, E. Brehat, and A. Hadni, Spectres d'absorption dans l'Infrarouge lointain d'un cristal pyroélectrique de saccharose (unpublished).